Journal of Magnetics 13(2), 70-75 (2008)

Enhancement of Magneto-optical Kerr Effect Signal from the Nanostructure by Employing Anti-reflection Coated Substrate

D.-H. Kim and Chun-Yeol You*

Department of Physics, Inha University, Incheon 402-751, Korea

(Received 21 May 2008)

In this study, a MOKE (Magneto-optical Kerr effect) measurement method for magnetic nanostructures is proposed. Theoretically, the MOKE signal enhancement can be predicted and confirmed when an anti-reflection coated substrate is used. Since MOKE is a ratio of reflectivity and the difference between the reflectivities for two magnetic states, when the reflectivity of the substrate part is reduced by employing an anti-reflection coated substrate, MOKE signal enhancement can be achieved. The enhancement is confirmed by simple numerical MOKE calculations. When the reflectivity of an anti-reflection coated substrate is 0.7%, the calculated MOKE signal is about 79% of its bulk values for the 100-nm wide Fe nanowire with a 1500-nm radius laser beam. It was found that, for various numerical calculations, a larger MOKE signal is obtained relative to a smaller substrate reflectivity.

Keywords : Magneto-optical Kerr effect, magnetic nanostructure, nanowire, nanodot

1. Introduction

Magnetic dynamics in ferromagnetic nanostructures in relation to nanodot and nanowire is one of the most exciting research areas [1, 2], because of its rich physics [3] and technical importance [4]. In order to study magnetic dynamics, fine spatial resolutions are required as well as ultrafast time resolutions. While there are various tools available for magnetic properties measurements, only a few of these provide both resolutions. For example, while PEEM (photoemission electron microscope) [5] and MTXM (magnetic transmission x-ray microscopy) [6] have excellent spatial and time resolutions, they are also types of stroboscopic (pump-probe) techniques. This means they can only measure the assemble average of physical phenomena, which requires reproducible processes. Furthermore, PEEM and MTXM are not available for most researchers.

MOKE (Magneto-optical Kerr effect) is another fine experimental tool used for the investigation of the magnetic dynamics of the ferromagnetic body. MOKE has an ultra-high sensitivity to a sub-monolayer [7]. Furthermore, an order of sub nano-second time can be used, thus resolving the power with pump probing technique [8], while the setup is relatively simple compared to that of other instrumental tools. However, MOKE has a poor spatial resolution for sub-microns because the beam spot size is restricted by the diffraction limit. According to classical optics, the beam spot size is in the order of $\sim\lambda/NA$, where NA is a numerical aperture of the lens, which is typically the order of the unit. Since the typical size of nanostructures is smaller than the beam spot size, this results in the unwanted degradation of the MOKE signal. In order to overcome the poor signal to noise ratio, Cowburn *et al.* [9] and Beach *et al.* [10] have taken numerous averages from raw data. Furthermore, when the beam spot size is excessively reduced, the nanostructure will become heated, and the uncertainty of the system temperature will prevent the correct interpretation of the observed data. Therefore, the MOKE has limited functionality for nanostructure measurement. If the spatial resolution of the MOKE can be enhanced, it can become an improved tool for magnetic dynamics studies.

While it is difficult to overcome the diffraction limit, over the past few decades many efforts have been made in various fields to prevail over the diffraction limit. One of the most promising techniques proposed is the Super-RENS (Super-Resolution-Near-Field-Structure) technique [11], which has been actively studied in the optical

*Corresponding author: Tel: +82-32-860-7667
Fax: +82-32-872-7562, e-mail: cyyou@inha.ac.kr

recording field. In this study, the key idea of the Super-RENS is adapted to the MOKE measurement system. Through this application, it is possible to bypass the diffraction limit in the MOKE measurement. Similar ideas have previously been experimentally and theoretically tested by numerous groups [12-16]. In this study, numerical calculations are performed for the enhancement of the MOKE for various beam spot sizes and sizes of nanostructures.

2. MOKE and Super-RENS

The concept of a magneto-optical Fresnel reflection matrix is useful to describe the MOKE phenomenon, and is defined as follows:

$$\Re = \begin{pmatrix} r_{ss} & r_{sp} \\ r_{ps} & r_{pp} \end{pmatrix}. \quad (1)$$

Here, r_{ij} ($i, j = s$ or p) is the reflectivity for the j-incident and i-reflected waves, so that the complex Kerr angles for s and p polarizations are defined as follows [17, 18]:

$$\theta_K^p = r_{sp}/r_{pp}, \quad (2)$$

$$\theta_K^s = r_{ps}/r_{ss}. \quad (3)$$

Using these definitions, it can be generally stated that the MOKE is the ratio between two reflected beams, r_{ij} and r_{ii}. Essentially, the MOKE can be demonstrated by the ratio between the change of the reflectivity due to the change of the magnetization ΔR and the reflectivity R, as follows:

$$\theta_K = \Delta R/R. \quad (4)$$

Hereafter, Eq. (4) will be used in this study as a definition of the MOKE rather than using more rigorous definitions. Before explaining the basic idea of this work, the Super-RENS technique, which is actively studied in the Optical Recording Society, needs to be elucidated [19]. Since the bit size of an optical disk is determined by the laser beam spot size, reducing the bit size is a most important issue for the Optical Recording Society. However, the reduction of the beam spot size is restricted by the diffraction limit of the light. To overcome this problem, it has introduced an additional aperture layer to the recording multilayer stack. An additional aperture layer that reduces reflectivity R plays a similar role to that of an antireflection-coated layer in a recording system. The aperture layer has a strong non-linear temperature dependent refractive index. When the laser beam is irradiated to the disk, the spatial temperature profile is related to the beam intensity profile, which is approximately a Gaussian distribution. Thus the temperature around the beam center has the highest value, and the aperture layer around the beam center has quite a different refractive index compared to that of the room temperature. As a result, the aperture layer can act as a dynamic aperture in which the size is significantly smaller than the beam size. In addition, when the thermally activated aperture is placed near the recording layer, it can be used as a type of near field source. Using this idea, the signal can be amplified from the beam center and suppressed from the circumference, and the diffraction limits can be surmounted. Further details regarding the Super-RENS technique can be found in other literature [19].

3. MOKE from a nanostructure on the Anti-reflection coated substrate

The rigorous vector diffraction theory and the near field optics framework must be applied to the optics for the nanostructure. Therefore, the exact MOKE signal from a nanostructure must be calculated using complex numerical calculations such as the magneto-optical FDTD (Finite Difference Time Domain) [20, 21]. However, in this case, a number of simple assumptions will be sufficient to distinguish the trend of the signal variations. For the sake of simplicity, only the magnitude of the MOKE is considered and it is assumed that the MOKE signal from a nanostructure can be described as follows:

$$\Theta_K^{\text{nano}} = \frac{\int I(x,y)\Delta R(x,y)}{\int I(x,y)R(x,y)}. \quad (5)$$

Here, R and ΔR represent each unit cell, and Θ_K^{nano} is the MOKE signal from the nanostructure. $I(x, y)$ is an intensity profile of the irradiated laser beam, which is Gaussian. Thus Eq. (5) can be written as,

$$\Theta_K^{\text{nano}} = \frac{\int I(x,y)\Delta R_{\text{nano}}(x,y)}{\int I(x,y)[R_{\text{sub}}+R_{\text{nano}}]}. \quad (6)$$

Here, R_{sub}, R_{nano} and ΔR_{nano} are reflectivities of the substrate, the nanostructure and the different reflectivity of nanostructure for each unit cell, respectively. Because the substrate is non-magnetic, there is no ΔR_{sub} from the substrate. One of the main sources of MOKE degradation from the nanostructure is the R_{sub} term. According to Eq. (6), R_{sub} is placed at the denominator, and when it is finite, Θ_K^{nano} is always smaller than the bulk value, $\Theta_K^0 = (\Delta R_{\text{nano}}/R_{\text{nano}})$. This is the key idea of this work. If an anti-reflection coated substrate is employed, a small value of R_{sub} can be obtained. In an ideal case (R_{sub}=0%), the MOKE signal will approach its bulk value. Fig. 1

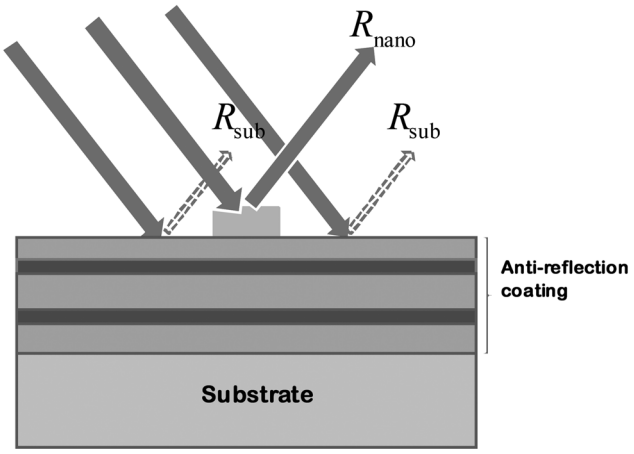

Fig. 1. Sketch of the concept of MOKE signal enhancement with anti-reflection coated substrate. The contribution to the MOKE from the beam irradiated on the anti-reflection coated substrate is minimized. The reflected beam on the substrate is illustrated by dashed arrows, which indicates that their intensities are small.

shows an illustration of this idea. The irradiated laser beam on the nanostructure has its bulk MOKE signal, while the beam on the substrate has a zero-MOKE signal and a very small reflection due to the antireflection coating. It should be emphasized here that calculations in this study are not exact, due to the simplification of the calculations. However, they do capture all important physics and the tendencies are quite correct.

Details of the calculation method will be explained in this paper. The problem space was divided by small cells in order to calculate the MOKE signal from the nanostructures. R and ΔR are calculated for each cell. The medium boundary and propagation matrix method [22] are used, and the results of each cell are summated with the Gaussian beam profiles as weight factors. The calculations in this study are performed with the following conditions. The wavelength is 632.8 nm (He-Ne laser), and the magnetic material is Fe with $\varepsilon_{xy} = 2.87+3.36i$. Here, ε_{xy} is the off-diagonal component of the dielectric tensor, which is the source of the MOKE. The incident angle of 45° is used for the *s*-polarization wave. The thickness of the Fe is 10-nm and the widths of the nanowire vary from 100 to 1500 nm. The radii of the beam spot vary from 100 to 1600 nm. The considered substrates consist of multilayer stacks in order to control the R_{sub} values.

4. Enhanced MOKE signal from nanostructures

In order to verify this idea, the MOKE signal is calcu-

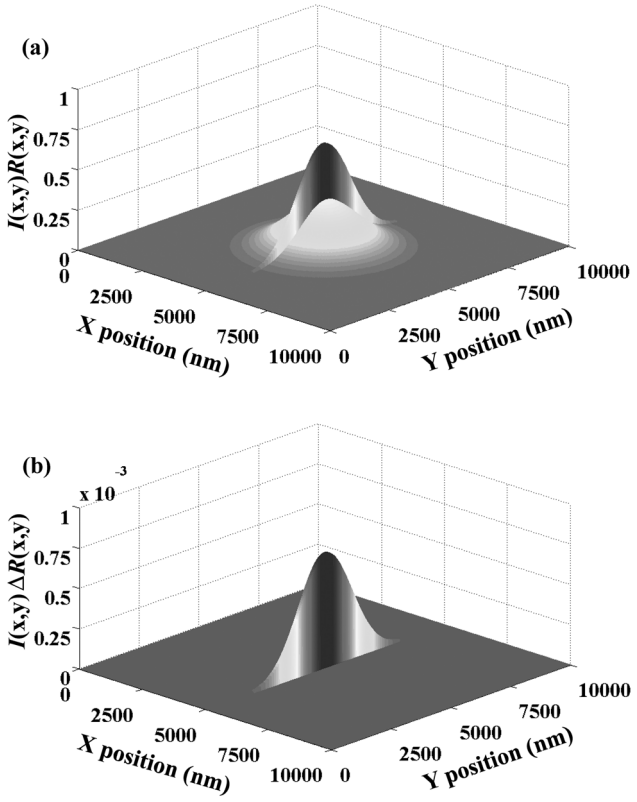

Fig. 2. (a) Denominator and (b) numerator of Eq. (5). 1.5-μm radius Gaussian beam is considered for 10 μm × 10 μm square substrate with 100-nm wide Fe nanowire for the case where R_{sub}=30%.

lated from the nanostructure for the two cases. In Fig. 2 (a) and 2(b), 3-dimensional plots for R and ΔR are shown for a typical glass substrate without an anti-reflection coating. The nanostructure is a 100-nm wide Fe layer and the beam radius is 1.5 μm. For R_{sub}=30% glass substrate, as expected the MOKE signal is only 7.1% of its bulk value. In order to examine the MOKE signal enhancement, an anti-reflection coated substrate is considered. With properly designed multilayer stacks, it is relatively straightforward to prepare a substrate of R_{sub}=0.7%. All of the conditions are the same as for the above case, with the exception of the substrate reflectivity. The results are presented in Figs. 3(a) and 3(b) and are, as expected, significant. The results of ΔR are almost identical to those shown in Fig. 2(b), while the results of R significantly differ to those shown in Fig. 2(a). As expected, the reflectivity of the substrate part is almost zero, implying that there is no contribution from the substrate in the MOKE measurement.

It should again be emphasized here that the calculation in this study is not rigorous. In a real case, there are some contributions to the MOKE signal from the vicinity of the

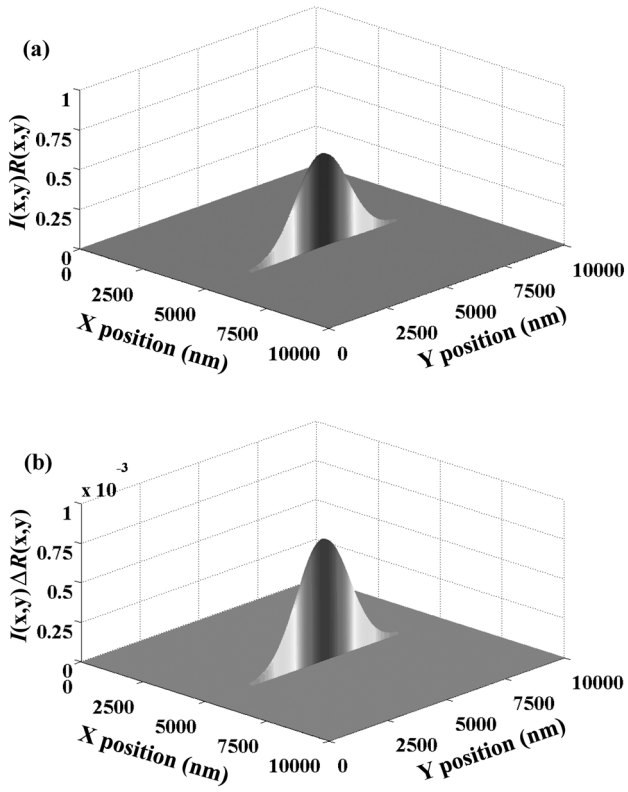

Fig. 3. (a) Denominator and (b) numerator of Eq. (5). 1.5-μm radius Gaussian beam is considered for 10 μm × 10 μm square substrate with 100-nm wide Fe nanowire for the case where R_{sub}=0.7%.

nanostructure when the exact diffraction theory is considered. Therefore, a type of maximum boundary of the enhancement effect is provided here.

5. Dependencies of the nanowire width and beam size

The MOKE signal dependencies of the nanowire width and the beam spot size are calculated. Fig. 4 shows the MOKE and normalized MOKE signals as a function of the wire width for four types of substrates with different reflectivities. The Gaussian beam radius is fixed at 1500 nm. It is assumed that the beam center and the nanowire center are matched. For the glass substrate (R_{sub}=30%) the MOKE signal for the 1500-nm wide nanowire has a normalized MOKE signal of 60% of its bulk value, and it decreases to ~10% for the 100-nm wide nanowire. However, when the substrate is anti-reflection coated (R_{sub}=0.7 %), the normalized signal for the 1500-nm wide nanowire is almost 100%. The normalized signal has retained its value of 100% up to when the nanowire width reaches 500 nm. For the 100-nm wide nanowire, the normalized MOKE signal is about ~79% of the bulk value. Two other

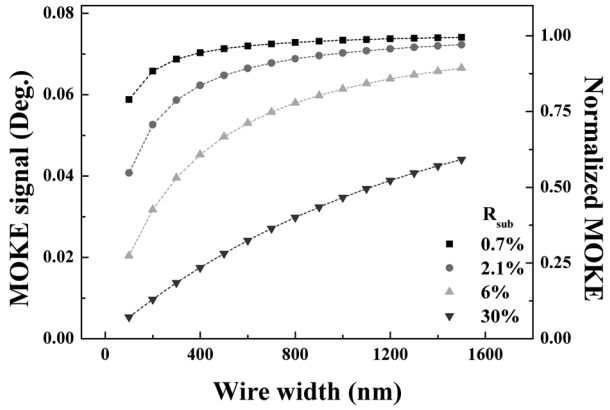

Fig. 4. MOKE and normalized MOKE signals are plotted as a function of the wire width for a 1500-nm radius Gaussian beam. Four different R_{sub} cases are considered.

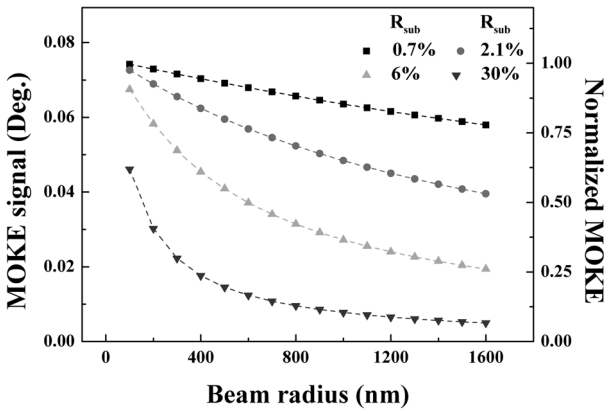

Fig. 5. MOKE and normalized MOKE signals are plotted as a function of beam radius for a 100-nm width Fe nanowire. Four different R_{sub} cases are considered.

cases are also plotted, of R_{sub}=6% and R_{sub}=21%. The dependence of the substrate reflectivity is clear. As expected, a superior MOKE signal can be obtained with a smaller R_{sub}. It should also be emphasized that, according to our previous calculations, the difference between the glass substrate and the anti-reflection coated substrate is about 7-8 times enhancement for 100-nm wide nanowire. In a real experiment, such enhancement is critical.

Fig. 5 depicts the dependence of the MOKE signal on the beam spot size for 100-nm wide Fe nanowire. The reflectivities of substrates R_{sub} of 0.7, 6, 21, and 30% are considered. When the beam radius is comparable to the wire width, the MOKE signal is closed to the bulk value, as shown in Fig. 4. In real experiments, such a small beam radius cannot be achieved due to the diffraction limit. When the beam radius increases, the signal is dropped. For the case where R_{sub}=30%, the signal decreases very rapidly. In particular, when the beam radius is larger than 900 nm, the normalized signals are less than 10%. Consi-

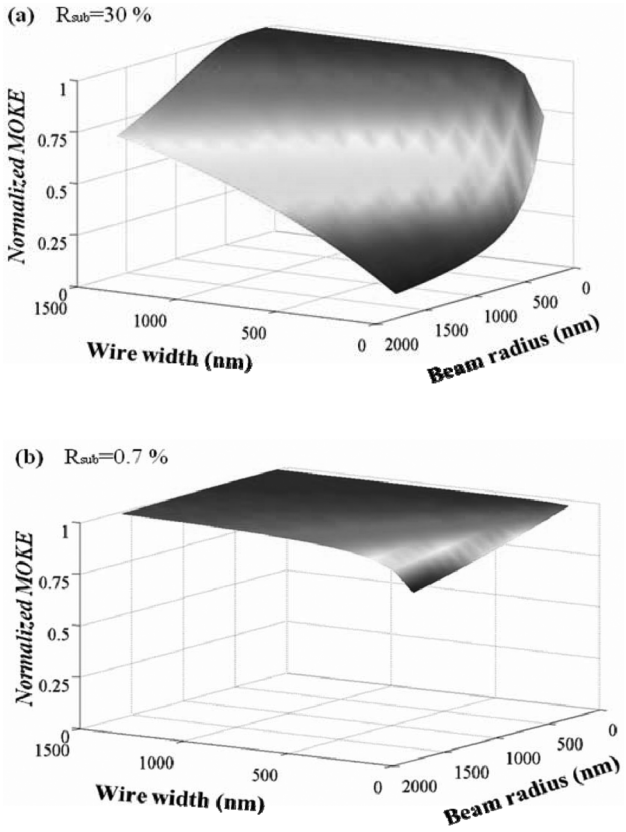

Fig. 6. MOKE signal of the two variables of wire width and beam radius are gradually increasing for (a) R_{sub}=30% and (b) R_{sub}=0.7%.

dering that a 900-nm radius is close to the experimental limit, the degradation of the signal is serious. However, for the case where R_{sub}=0.7%, the calculation results are more optimistic. For a 1500-nm beam radius, the normalized MOKE signal is 79%. For an even larger beam spot, the slope of the decrement is small. The cases where R_{sub} =6% and 2.1% show the intermediate results. Therefore, it can be concluded that if the reflectivity of the substrate is reduced, then the MOKE signal can be increased.

For further study of nanowire width and beam size variations, 3-dimensional maps are calculated, where the nanowire width is changed from 0 to 1500 nm and the beam size from 0 to 1600 nm, as shown in Figs. 6(a) and (b). For the case where R_{sub}=30%, the degradation of the MOKE signal is significant, as mentioned previously. It approaches ~10% of its bulk values for typical experimental conditions. However, for the case where R_{sub}=0.7 %, the degradation is very week, as shown in Fig. 6(b).

In real experiments, a perfect anti-reflection condition is either very difficult or impossible to obtain, depending on the substrates. However, the reducing reflectance is simply achieved by a single additional dielectric layer deposition. Fig. 7 shows the dependence of the MOKE signal on

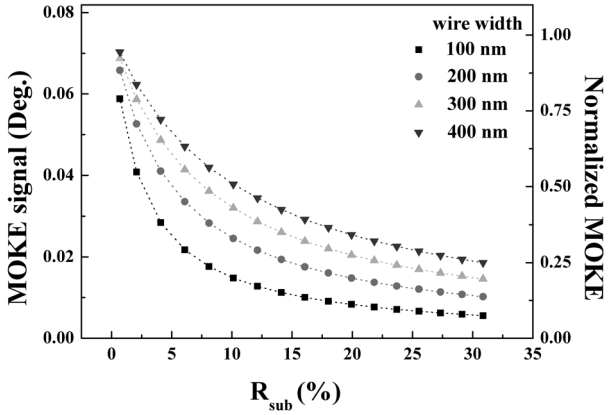

Fig. 7. MOKE and normalized MOKE signals are plotted as a function of R_{sub}. Four different nanowire widths are shown.

the R_{sub}. The beam radius of 1500 nm is considered, and the cases where the wire width is 100, 200, 300 and 400 nm are taken into account. From a simple expression of MOKE, as in Eq. (6), it is clear that when R_{sub}=0%, the MOKE value will approach its bulk values. Eq. (6) can generally be rewritten in a simpler form without consideration of the Gaussian beam profiles,

$$\Theta_K^{nano} \propto \frac{\Delta R_{nano}}{R_{sub} + R_{nano}} = \frac{\Delta R_{nano}/R_{nano}}{1 + R_{sub}/R_{nano}} = \frac{\Theta_K^0}{1 + R_{sub}/R_{nano}}. \quad (7)$$

Using Eq. (7), the decrement behavior of the MOKE signals in Fig. 7 can be easily understood. It should be noted here that there is no information for the wire width and beam radius in Eq. (7). The curves in Fig. 7 must therefore be merged to a single curve. These discrepancies are ascribed to the overly crude approximation of Eq. (7), which is derived without consideration of the Gaussian beam profiles.

6. Conclusions

It is found that the MOKE signal from nanostructures can be enhanced by tailoring the substrate reflectivity. With the anti-reflection coating of the substrate the reflected beam can be suppressed from the non-magnetic substrate. Since a physical meaning of the MOKE is $\Delta R/R$, with a reduction of R from the substrate part, the enhancement of the MOKE signal can be achieved. The presented method can be applied to all types of nanostructures, and the enhancement of MOKE will be very helpful for magnetic nanostructure research.

Acknowledgements

This work is supported by KOSEF (Basic Research

Program No. R01-2007-000-20281-0).

References

[1] Joonyeon Chang, A. A. Fraerman, Suk Hee Han, Hi Jung Kim, S. A. Gusev, and V. L. Mironov, J. Magnetics **10**(2), 58 (2005).
[2] Ji-sang Hong, J. Magnetics **11**(1), 20 (2006).
[3] Luc Thomas, M. Hyayashi, X. Jiang, R. Moriya, C. Rettner, and S. Parkin, Science **315**, 1553 (2007).
[4] S. S. P. Parkin, US. Patent No. 6834005 (2004).
[5] S.-B. Choe, Y. Acremann, A. Scholl, A. Bauer, A. Doran, J. Stöhr, and H. A. Padmore, Science **304**, 420 (2004).
[6] G. Meier, M. Bolte, R. Eiselt, B. Krüger, D.-H. Kim, and P. Fischer, Phys. Rev. Lett. **98**, 187202 (2007).
[7] D. A. Allwood *et al*., J. Appl. Phys. **95**, 8264 (2004).
[8] J.-Y. Bigot, L. Guidoni, E. Beaurepaire, and P. N. Saeta, Phys. Rev. Lett. **93**, 077401 (2004).
[9] D. A. Allwood, G. Xiong, M. D. Cooke, C. C. Faulkner, D. Atkinson, N. Vernier, and R. P. Cowburn, Science **296**, 2003 (2002).
[10] G. S. D. Beach, C. Nistor, C. Knutson, M. Tsoi, and J. L. Erskine, Nat. Mat. **4**, 741 (2005).
[11] J. Tominaga, T. Nakano, and N. Atoda, Appl. Phys. Lett. **73**, 2078 (1998).
[12] D. A. Allwood, Gang Xiong, M. D. Cooke, and R. P. Cowburn, Appl. Phys. **36**, 2175 (2003).
[13] L. F. Holiday and U. J. Gibson, OPTICS EXPRESS **14**, 13007 (2006).
[14] Ursula. J. Gibson, Lindsay F. Holiday, Dan A. Allwood, Swaraj Basu, and Paul W. Fry, IEEE Trans. Magn. **43**, 2740 (2007).
[15] P. R. Cantwell, U. J. Gibson, D. A. Allwood, and H. A. M. Macleod, J. Appl. Phys. **100**, 093910 (2006).
[16] Naser Qureshi, Suqin Wang, Mark A. Lowther, Aaron R. Hawkins, Sunghoon Kwon, Alexander Liddle, Jeffrey Bokor, and Holger Schmidt, Nano Lett. **5**, 1413 (2005).
[17] C.-Y. You and S.-C. Shin, J. Appl. Phys. **84**, 541 (1998).
[18] C.-Y. You and S.-C. Shin, J. Mag. Mag. Mater. **198**, 573 (1999).
[19] See, Tech. Digests of Int. Symp. Optical Memory and Optical Data Storag.
[20] Y. He, T. Kojima, T. Uno, and S. Adachi, IEICE Tran. Elec. **E81-C**, 1881 (1998).
[21] J. Liu, B. Xu, and T. C. Chong, Jpn. J. Appl. Phys. **39**, 687 (2000).
[22] J. Zak, E. R. Moog, C. Liu, and S. D. Bader, Journal of Magnetism and Magnetic Materials **89**, 107 (1990).